Available online at www.sciencedirect.com
ScienceDirect
Polymer 48 (2007) 5332–5339
polymer
www.elsevier.com/locate/polymer

Effect of clay treatment on structure and mechanical behavior of elastomer-containing polyamide 6 nanocomposite

Ivan Kelnar [a,*], Viera Khunová [b], Jiří Kotek [a], Ludmila Kaprálková [a]

[a] *Institute of Macromolecular Chemistry AS CR, v.v.i., Heyrovsky Sq. 2, 162 06 Prague, Czech Republic*
[b] *Department of Plastics and Rubber, Faculty of Chemical and Food Technology, Slovak University of Technology, Radlinského 9, Bratislava, Slovak Republic*

Received 23 March 2007; accepted 22 June 2007
Available online 4 July 2007

Abstract

The effect of clay organophilization on mechanical behavior and structure of PA6/EPR blends was studied. It has been shown that the modification of clay affected simultaneously the degree of PA6 matrix reinforcement, size and structure of dispersed EPR. The localization of clay with less polar treatment in the interfacial area brought an important new effect consisting intensification of toughening effect of dispersed elastomer by formation of ''core–shell'' particles. Basic aspects governing formation of this advantageous structure are reported.

The best balanced mechanical behavior was achieved when combining two differently modified clays, whereas the clay with less polar treatment is preblended with EPR. In this way, a high degree of matrix reinforcement (exfoliation of clay with more polar treatment) was combined with favorable size and structure of dispersed EPR phase. Additionally, at lower clay content, synergy between clay and elastomer phase, monitoring itself by enhancement of toughness, was found.

Keywords: Immiscible polymer blend; Compatibilization; Organoclay

1. Introduction

An increasing amount of papers indicates that nanoscale-layered silicates can impart not only a significant reinforcement [1] to single polymer phases but also can affect the dynamic phase behavior and thus morphology of immiscible polymer blends. Usually a decrease in dispersed phase size is reported [2–16]. The compatibilizing effect and resulting properties depend on clay localization and degree of its dispersion, which is determined by the clay–polymer component affinity [2,3]. A marked effect of clay on refinement of dispersed phase was found in the case of presence of clay in the matrix phase and at the interface, limiting the coalescence due to an interfacial active role of clay. The effect of the changed viscosity ratio [4,5] is also important. Reduction in particle size was observed also in blends with clay dispersed in matrix phase only [6–9]. According to Bousmina et al. [10], the anisotropic clay dispersed in the matrix acts as an effective barrier, which prevents the deformation and coalescence of the dispersed phase. This type of clay distribution leads also to higher toughness of elastomer-modified nanocomposites because the clay dispersed in the elastomer phase decreases its cavitation ability [11]. Similar trends were observed also in some thermoplastic elastomers [12]. A decrease in particle size was found further in comparable dispersion of clay in both phases [2,13–15], mainly in the case of low dispersion of clay within polymer constituents, when the clay is localized in the interfacial area. According to Wang et al. [16], the compatibilizing effect originates from cointercalation of both polymers into clay tactoids (leading to the compatibilizer formation). On the other hand, antagonistic effects such as coarsening of particle size by clay addition were found for

* Corresponding author. Tel.: +420 296 809 365.
E-mail address: kelnar@imc.cas.cz (I. Kelnar).

0032-3861/$ - see front matter © 2007 Elsevier Ltd. All rights reserved.
doi:10.1016/j.polymer.2007.06.062

systems with clay incorporated preferentially within the dispersed phase [17–20] (PP matrix/PA6). This phenomenon, preferential wetting of one (dispersed) phase and hard particles impeding the growth of the domains, was simulated by Balasz et al. [21]. An increase in domain size by clay addition was found also for some reactively compatibilized systems [22–24]. At the same time, Dharayia and Jana [25] found a decrease in size of PP particles with preblended clay dispersed in the PA6 matrix. It was found that clay particles residing in fibrils (formed from original large PP particles) dictated the ''wavelength'' of capillary instability and resulted in droplets similar in size to the size of clay particles. In PPO/PA [26] and PA6/ABS [27] blends, addition of clay supported co-continuous structure formation. Addition of clay to PPS/PA66 blend caused shift of phase inversion [28]. Si et al. [29] and Bousmina et al. [10] have found enhanced miscibility between blend components caused by clay. Combination of dispersed elastomer phase and clay may also lead to synergistic enhancement of mechanical behavior as it was found for PVC or PA systems [30–33]. In the case of clay localized in the interfacial region, both modification of interface parameters and formation of ''core–shell'' particles (with outer shell consisting of multiple silicate layers) may occur [33,34]. Our recent study on toughened PA6 nanocomposites indicated that the formation of the ''core–shell'' impact modifier structure is the reason for fair balance of mechanical properties and, moreover, the addition of clay to elastomer-containing PA6 even enhanced toughness [33]. Additionally, clay-compatibilized systems containing nonreactive elastomers showed higher mechanical performance than analogous systems with reactive elastomers. Based on these results, the present work is focused on the effect of the affinity of the clay and polymer components on the structure and mechanical behavior of elastomer-containing PA6 systems. Various elastomers in combination with clays with different organophilization as well as different preparation procedures are applied aimed at description and elucidation of reinforcing and compatibilizing effects of clay. The paper brings new fundamental understanding of the complex effect of nanofiller in rubber modified polyamide nanocomposites.

2. Experimental

2.1. Materials

Polyamide 6 (PA6) Ultramid B5, BASF, $M_n = 42\,000$; Maleated (0.6%) ethene-propene elastomer (EPR-MA) Exxelor 1801, Exxon Mobil; Ethene-propene elastomer (EPR) Buna AP 331, Degussa Hüls, Germany; Ethene-methyl acrylate copolymer (EMA) Lotril 28MA07 (30% MA); Hydrogenated butadiene-acrylonitrile copolymer (NBR), Breon N 33, Nippon Zeon; the used clays based on natural montmorillonite (MMT) (Southern Clay Products, Inc.) are shown in Table 1.

2.2. Nanocomposite preparation

Prior to mixing, PA6 and clay were dried at 85 °C and 70 °C, respectively, for 12 h in a vacuum oven. The blends were prepared by mixing the components in the W 50 EH chamber of a Brabender Plasti-Corder at 255 °C and 45 rpm for 10 min. The material was immediately compression-molded at 250 °C to form 1-mm thick plates. Strips cut from the plates were used for preparation of dog-bone specimens (gauge length 40 mm) in a laboratory micro-injection molding machine (DSM). The barrel temperature was 265 °C and the mold temperature was 80 °C.

2.3. Testing

Tensile tests were carried out at 22 °C using an Instron 5800 apparatus at a crosshead speed of 20 mm/min. At least 8 specimens were tested for each sample. The stress-at-break,

Table 1
Characteristics of clays

Cloisite 15A	Cloisite 20A	Cloisite 25A
Modifier concentration: 95 meq/100 g; anion: chloride	Modifier concentration: 125 meq/100 g; anion: chloride	Modifier concentration: 95 meq/100 g; anion: methyl sulfate
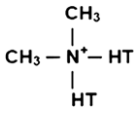	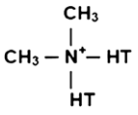	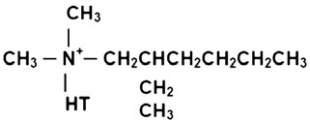
Cloisite 93A Modifier concentration: 90 meq/100 g; anion: HSO_4	Cloisite 30B Modifier concentration: 90 meq/100 g; anion: chloride	
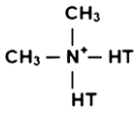	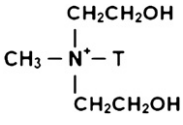	

HT is hydrogenated tallow; the alkyl composition: ~65% C18, ~30% C16 and ~5% C14.

σ_b, elongation at break, ε_b, and Young's modulus, E, were evaluated. Corresponding variation coefficients do not exceed 2%, 15% and 5%, respectively.

Tensile impact strength, a_t, was measured with one-side notched specimens, using a Zwick hammer with an energy of 4 J (variation coefficient 10–15%). The reported values are averages of 12 individual measurements.

A Perkin–Elmer Pyris 1 DSC apparatus was used for calorimetric measurements. Thermograms were scanned in the temperature interval 80–260 °C at the heating rate 10 °C/min.

2.4. Morphological observations

Phase structure was observed on cryo-fractured samples using scanning electron microscopy (SEM). The elastomer phases were etched with *n*-heptane for 1 h or with boiling xylene for 2 min. The size of dispersed particles was evaluated from their micrographs using a MINI MOP image analyzer (Kontron Co., Germany). For transmission electron microscope (TEM) observations, ultrathin (60 nm) sections were cut, under liquid N_2, from a stained (RuO_4 vapor for 90 min) sample using an Ultracut UCT (Leica) ultramicrotome.

Wide-angle X-ray diffraction (XRD) patterns were obtained with a powder diffractometer HZG/4A (Freiberger Präzisionsmechanik GmbH, Germany) and monochromatic Cu Kα radiation.

3. Results and discussion

3.1. Effect of clay organophilization

Results in Table 2 indicate a significant effect of the clay organophilization type on mechanical behavior and size of dispersed phase. This is particularly pronounced for PA6/EPR with lowest compatibility. In this case, the most significant compatibilizing effect was found for the clay modified with tallow only, i.e., C15A and C20A, see Table 2 (treatment with lower polarity and thus higher affinity to EPR). A similar trend with less significant differences in particle size was found for more polar (and compatible with PA6) ethene-methyl acrylate copolymer (EMA). Conversely, with significantly more polar NBR, finer particles were found for C30B, containing, in addition to tallow, also two 2-hydroxyethyl groups (Table 2).

As expected, the significantly finer elastomer dispersion of EPR elastomers leads to enhancement of toughness (Table 2). In the case of EMA and NBR, which are more compatible with PA6, already the initial size of particles (in the absence of clay) seems to be closer to optimal one; therefore, differences in toughness are less significant. Furthermore, the most decisive factor determining strength and stiffness is the degree of clay exfoliation. XRD patterns in Fig. 1 indicate a lower degree of exfoliation of clays with less polar treatment (C15A and C20A) in the PA6 matrix, which tends to decrease the strength and stiffness (Table 2) of corresponding nanocomposite. As a result, the clay with the best compatibilizing effect does not lead to the best balance of mechanical behavior. The solution to this problem is demonstrated in the last part of this paper.

A significantly higher compatibilizing efficiency of C15A in comparison with C30B in the PA6/EPR system is best visible in the dependence of particle size on the clay concentration as shown in Fig. 2. The effect of both clays (C15A and C30B) on the decrease in the EPR particle size is markedly pronounced already at low clay contents. The dependences for both clays represent emulsification curves. The absence of saturation even at relatively high clay contents (when the clay content exceeds the EPR content, but a majority of clay is still dispersed within the matrix) could be ascribed to viscosity enhancement due to clay [35] and change in the mechanism of particle generation during mixing [10].

Table 2
Effect of clay treatment on mechanical behavior and particle size for nanocomposite containing 5%

Composition	σ_b (MPa)	E (MPa)	a_t (kJ m^{-2})	Particle size (nm)	ε (%)
EPR					
PA6/C30B/EPR	88.5	2650	31	600	140
PA6/C15A/EPR	75	2220	66.5	360	80
PA6/C20A/EPR	75	2270	36	370	190
PA6/C25/EPR	83.5	2420	46	400	160
PA6/C93A/EPR	86	2320	49.5	500	70
NBR					
PA6/C30B/NBR	85	2450	64.5	220	55
PA6/C15A/NBR	76	2040	52	350	195
PA6/C25/NBR	84.5	2430	68.5	250	190
EMA					
PA6/C30B/EMA	86.5	2540	61	180	170
PA6/C15A/EMA	76.5	2220	44	150	70
PA6/C20A/EMA	78.5	2300	63.5	110	75
PA6/C25/EMA	85.5	2510	43	130	155

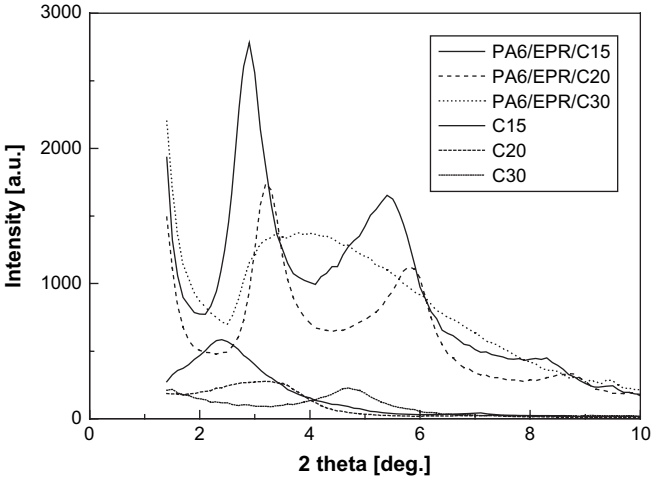

Fig. 1. XRD patterns of a nanocomposite with 5% EPR containing clays with different organophilization.

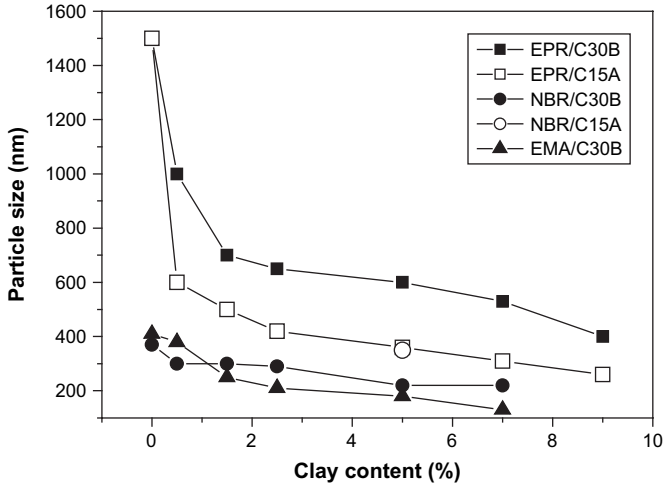

Fig. 2. Effect of clay concentration on particle size of dispersed EP.

These effects seem to be dominant especially for nanocomposites containing C30B (in agreement with Ref. [7]) due to the absence of clay in the interfacial region and also in the dispersed EPR (Fig. 3a, Ref. [33]), indicating that the interfacial activity of clay cannot be considered in this case (clays do not act as ''classical'' compatibilizers). In the case of systems containing clay with less polar treatment (C15A or C93A), the more pronounced decrease in particle size seems to be mainly a consequence of simultaneous clay localization at the interface (Fig. 3b), representing the ''true compatibilizing effect'' with expected co-intercalation and/or absorption of both polymers and clay in the interfacial region [2,16]. It can be observed in Fig. 3c that with higher C30B content (9%), the clay is localized also at the interface, probably due to an excess of clay over the amount necessary to form the percolated clay-network [36]. This additional compatibilizing effect is reflected in a significant particle size decrease between the 7% and 9% C30B contents in comparison with analogous nanocomposite containing C15A (Fig. 2), having already clay at the interface.

From Fig. 2 it is also evident that the decrease in the size of NBR particles by clay is less pronounced, undoubtedly as a result of significant compatibility indicated by a low particle size (about 370 nm) in binary blend PA6/NBR. For NBR, well-developed structures of clay-surrounded particles [33] were found for all the clay treatments used (due to similar polarity of both constituents and thus also affinity to clay). The only difference was a slightly lower regularity of this clay layer (envelope) for the C15A clay with less polar treatment (not shown). The finer particle size (Fig. 2) found for the C30B-containing system seems to be mainly a consequence of the expected higher matrix viscosity and stronger interaction of clay localized at the interface with both polymers.

The above results indicate that more effective (and ''true'') compatibilizing occurs in the case of clay localized at the interface. For PA6/EPR, this structure can be achieved with modified clays with higher affinity to the dispersed phase. On the other hand, the affinity to the dispersed phase should not exceed significantly the affinity to matrix, since presence and/or exfoliation in the dispersed phase lead to structure coarsening [17–21].

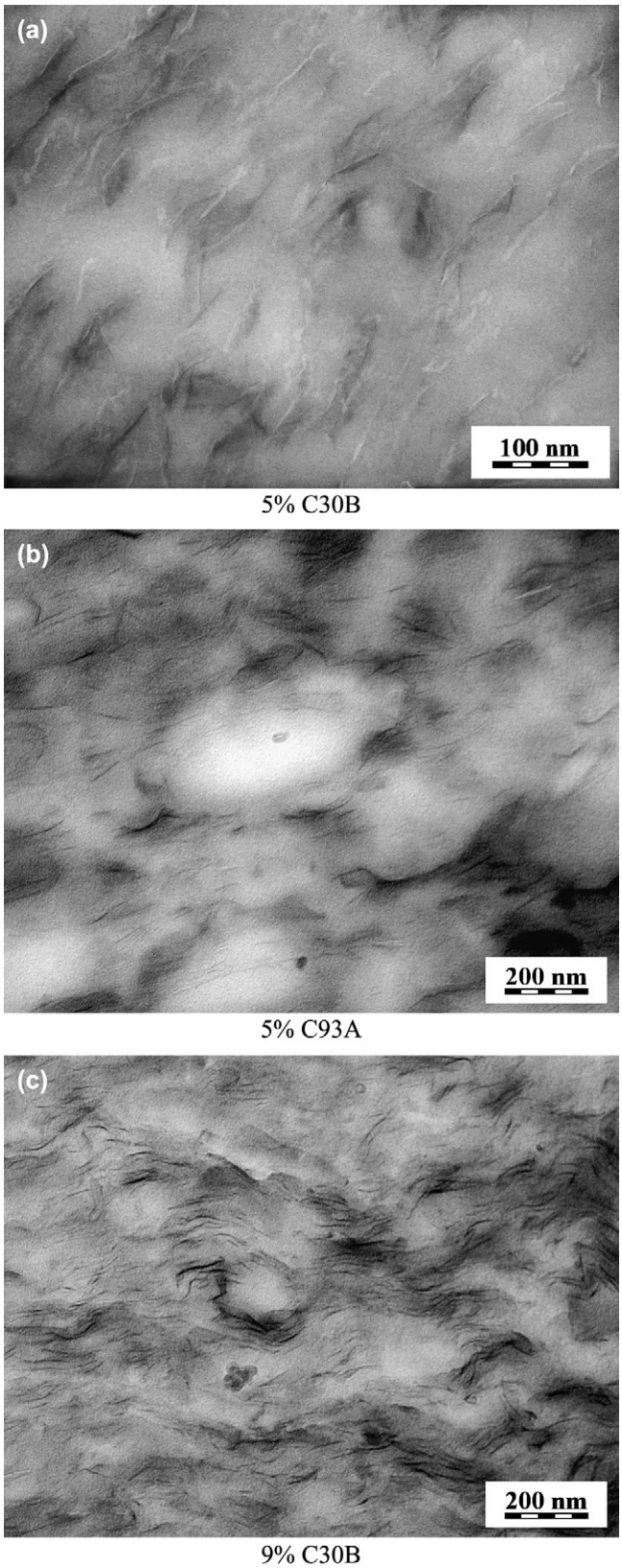

Fig. 3. TEM observation of a nanocomposite containing 5% of elastomer.

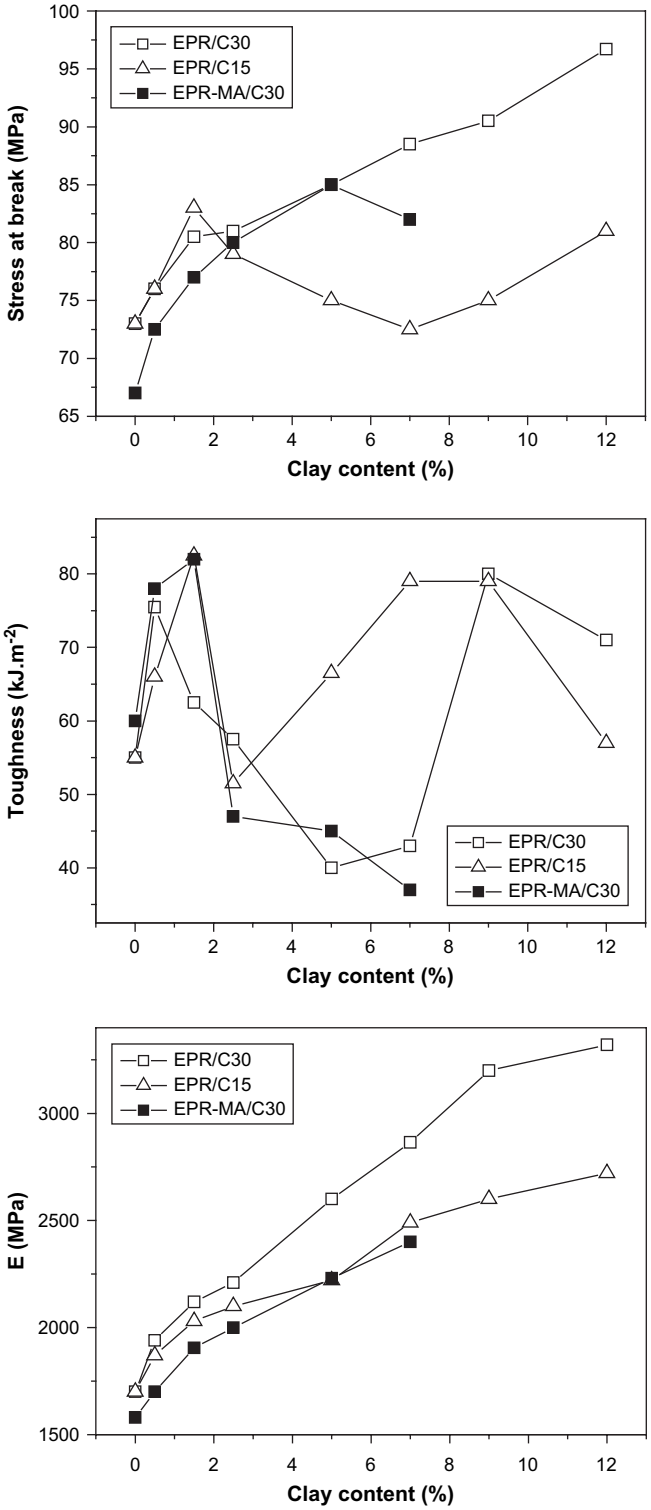

Fig. 4. Mechanical properties of a nanocomposite containing 5% of elastomer in dependence on clay type and content.

Fig. 4 shows mechanical properties in dependence on increasing clay content for nanocomposites containing EPR and EPR-MA. Addition of low amounts of C15A or C30B clays causes a significant toughness enhancement indicating a certain synergy between clay and elastomers. According to XRD (not shown) and DSC (Fig. 5), the main effect of increasing clay content on the crystallinity of PA6 with 5% EPR is a corresponding increase in the γ phase content, typical also of neat PA6 nanocomposite. The overall crystallinity varies only insignificantly – no marked change in crystallinity at low clay contents, corresponding to the above mentioned maximum of toughness, was observed. Therefore, a tentative explanation may be the more favorable ratio of moduli of dispersed rubber and PA6 matrix and also minor changes in matrix crystallinity.

In the case of EPR-containing nanocomposite, the effect of both clay types on toughness at concentrations exceeding 1.5% is different. Whereas for C30B, the toughness is significantly decreasing up to 7% content (which is rather surprising due to simultaneous decrease in particle size), the toughness of C15A-containing nanocomposite reaches a significantly higher level especially for the 5% and 7% clay contents. The explanation is based on different morphologies. Fig. 3 indicates the significant presence of lamellar stacks of clay around EPR particles for C15A (more distinct with increasing clay concentration). Such a kind of effective "core–shell" structure was found to be decisive for well-balanced mechanical behavior, especially for enhanced toughness, as was already observed for EMA-containing PA6 nanocomposites [33]. At the same time, a positive effect of lower matrix rigidity due to less exfoliated clay may be excluded (see Section 3.2 below). Similarly, Balakrishnan et al. [37] have found toughness enhancement of epoxy/MMT nanocomposites modified with preformed acrylic rubber caused by the presence of clay stacks at the rubber/epoxy interface. In the case of C30B, in the same range of the clay content (up to 7%), MMT is not present in the interfacial area (Fig. 3, Ref. [33]). From Fig. 4 it is further obvious that at higher content (9%) of C30B, an increase in toughness occurs. This is undoubtedly a consequence of the above mentioned occurrence of clay in the interfacial area (Fig. 3). This structure further supports the high effectivity of "core–shell" particles on toughening. The explanation of this effect, which most probably enhances the energy-absorbing capacity of the plastically deformed zone around rubber particles (or may even support rubber cavitation as proposed for epoxy nanocomposite [37]), needs further work.

In EPR-MA-containing nanocomposite, the increasing clay content causes a rather minor increase in particle size (from 60 nm to ~100 nm, Ref. [33]). Similar behavior was found also by other authors [22–24], probably due to blocking of reactive compatibilization leading to its original, very small size of 60 nm. More important is the simultaneous presence of a layer of single clay platelets at the surface [33], which suppresses (already hindered) cavitation of these very fine particles [38].

The lower values of strength and modulus for PA/EPR/C15A in comparison with PA/EPR/C30B then correspond with the above mentioned lower exfoliation of C15A in PA6 matrix (Fig. 1). On the other hand, a lower level of both parameters for systems with EPR-MA is a consequence of lowering of matrix crystallinity by reactively formed copolymer (compatibilizer) [39].

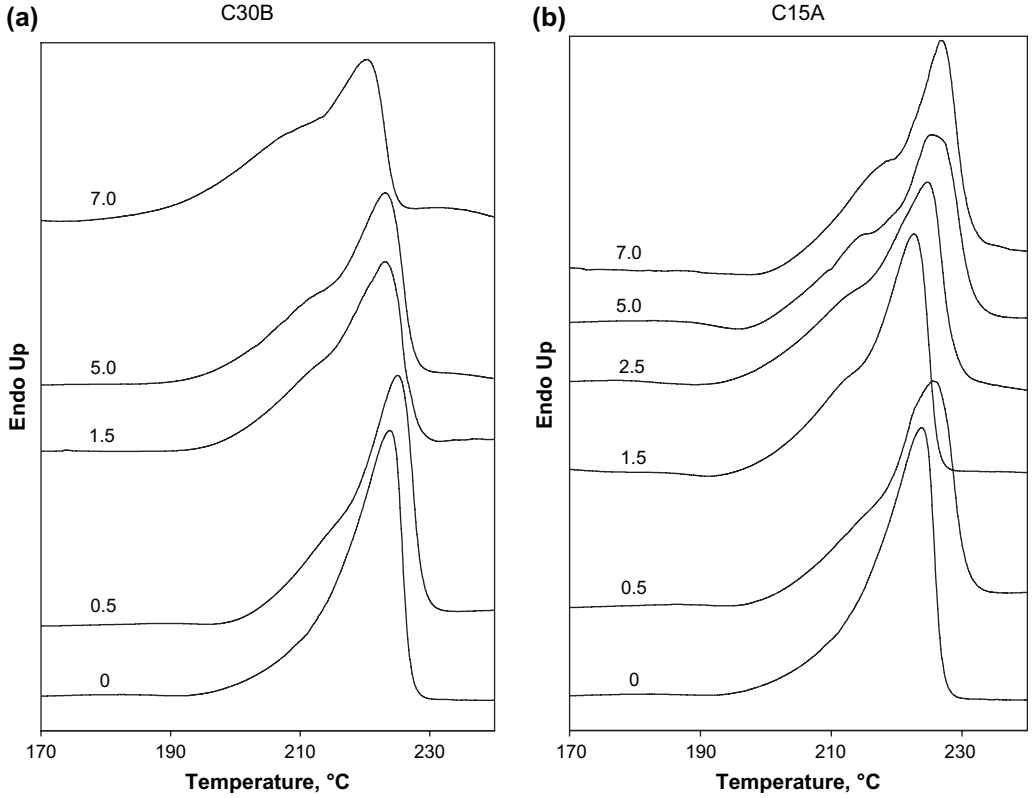

Fig. 5. DSC heating scans of nanocomposites containing 5% of EPR in dependence on the clay type and content.

3.2. Combination of two clays

From the above results it is clear that for EPR-containing nanocomposite, a simultaneous high delamination of clay in the PA matrix and a high compatibilizing effect (i.e., presence of clay at the interface) cannot be achieved using one type of clay treatment. To achieve a high level of both effects in one system, we combined two differently treated clays; C15A with less polar organophilization (in the amount respective to the EPR content) and more polar C30 (amount related to the PA6 matrix). Table 3 shows properties and particle size of PA6/EPR/clay systems mixed in one-step or using preblending of a less polar clay with rubber in the first step and following by mixing with the polyamide.

The best balanced mechanical behavior was found for preblended systems. The significantly finer structure of preblended samples is documented in Fig. 6, also TEM (Fig. 7) shows an advantageous well-developed structure of rubber particles surrounded by stacks of clay platelets. These results indicate that the two-step mixing protocol for a system containing two different clays leads undoubtedly to combination of high reinforcement, compatibilization effect and favorable ''core–shell'' structure.

The results in Table 3 further indicate that this method (preblending of elastomer with C20A) leads also to the best balanced behavior of an analogous EMA-containing system but with a less marked difference from other systems due to the above mentioned higher compatibility of both polymer components.

Table 3
Effect of combination of 2 clays and preblending on particle size and mechanical properties

Composition	σ_b (MPa)	E (MPa)	a_t (kJ m^{-2})	Particle size (nm)	ε (%)
90/5/5					
PA6/C30/EPR	89	2650	31	600	140
PA6/C15/EPR	75	2220	66.	360	80
PA6/(EPR/C15-5)pb/C30[a]	81.	2520	70	380	175
PA6(EPR/C15-10)pb/C30[b]	87	2560	105	280	183
PA6/C30/C15(0.8%)/EPR[c]	83	2510	35	550	11
90/5/10					
PA6/C30/EPR	76	2250	61	750	40
PA6/(EPR/C15-10)pbC30[b]	71	2210	63	370	106
90/5/5					
PA6/C30/EMA	87	2540	58	180	170
PA6/C25/EMA	86	2510	43	130	155
PA6/C15/EMA	77	2220	44	150	70
PA6/C20/EMA	79	2300	64	110	90
PA6(EMA/C20-10)/C30[d]	85	2630	68	130	155

[a] Preblend EPR/C15A 95/5.
[b] EPR/C15A 90/10.
[c] Simultaneous mixing, composition identical to 90/10 preblend.
[d] Preblend EPR/C20A 90/10.

4. Conclusions

The obtained results indicate that clays affect both the size and structure of the dispersed elastomeric phase. The second effect – formation of ''core–shell'' particles due to

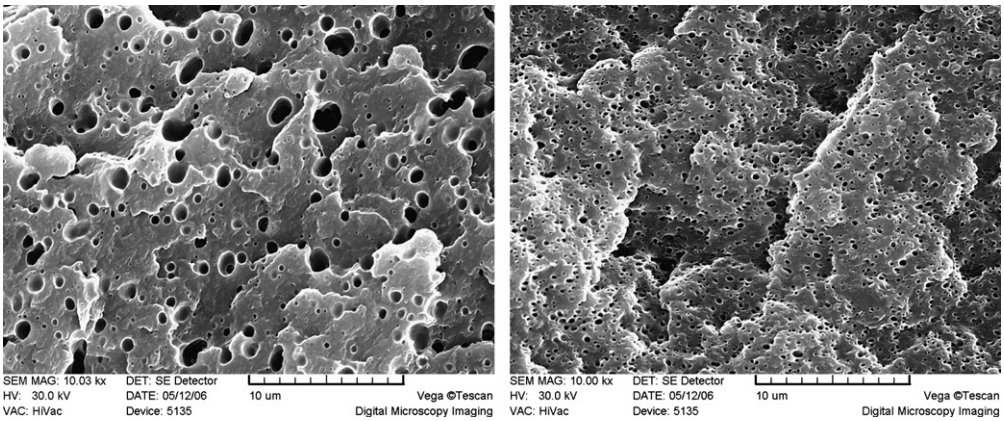

Fig. 6. Effect of EPR/C15A preblending; (a) PA6/C30B/EPR 85/5/10, one-step mixing and (b) PA6/(EPR/C15A)/C30B 85/(5)/10, EPR preblended with C15A in the ratio 90/10.

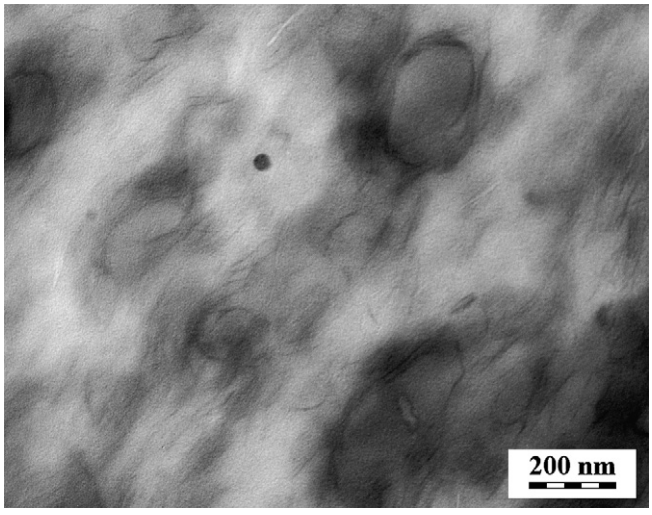

Fig. 7. TEM of nanocomposite with EPR/C15A (90/10) preblend (PA6(EPR/C15A)pb/C30B 90/5/5).

localization of clay with suitable treatment at the interfacial area leads to toughness enhancement. This new effect of clay was successfully combined with high matrix reinforcement when clays with different treatment were applied and the clay with less polar treatment was preblended with the elastomeric component.

In this way, a high degree of matrix reinforcement (exfoliation of the clay with more polar treatment) was combined with the favorable size and structure of the dispersed EPR phase. In addition, at lower clay contents, synergism of the clay and elastomer phase, reflected by enhancement of toughness on clay addition, was found.

Acknowledgment

The authors thank the Grant Agency of the Czech Republic (Grant no. 106/06/0044) and Grant Agency of the Academy of Sciences of the Czech Republic (Grant no. B200500601) for financial support.

References

[1] Pinnavaia TJ, Beall GW, editors. Polymer–clay nanocomposites. New York: John Wiley & Sons; 2001.
[2] Ray SS, Pouliot S, Bousmina M, Utracki LA. Polymer 2006;45:8403–13.
[3] Ray SS, Bousmina M. Macromol Rapid Commun 2005;26:1639–46.
[4] Gelfer MY, Song HH, Liu L, Hsiao BS, Chu B, Rafailovich M, et al. J Polym Sci B 2003;41:44–54.
[5] Chow WS, Mohd Ishak ZA, Karger-Kocsis J. Macromol Mater Eng 2005;290:122–7.
[6] Too Y, Park Ch, Lee S-G, Choi K-Y, Kim DS, Lee JH. Macromol Chem Phys 2005;206:878–84.
[7] Khatua BB, Lee DJ, Kim HY, Kim JK. Macromolecules 2004;37:2454–9.
[8] Lee H, Fasulo PD, Rodgers WD, Paul DR. Polymer 2005;46:11673–89.
[9] Voulgaris D, Petridis D. Polymer 2002;43:2213–8.
[10] Ray SS, Bousmina M, Maazouz A. Polym Eng Sci 2006;46:1121–9.
[11] Dasari A, Yu Z-Z, Mai Y-W. Polymer 2005;45:5986–91.
[12] Maiti M, Bandyopadhyay A, Bhowmick AK. J Appl Polym Sci 2006;99:1645–56.
[13] Ray SS, Bousmina M. Macromol Rapid Commun 2005;26:450–5.
[14] Mehta S, Mirabella FM, Rufener K, Bafna A. J Appl Polym Sci 2004;92:928–36.
[15] Essawy H, El-Nashar D. Polym Test 2004;23:804–7.
[16] Wang Y, Zhang Q, Fu Q. Macromol Rapid Commun 2003;24:231–5.
[17] Gahleitner M, Kretzschmar B, Van Vliet G, Devaux J, Pospiech D, Bernreitner K, et al. Rheol Acta 2006;45:322–30.
[18] Gahleitner M, Kretzschmar B, Pospiech D, Ingolic E, Reichelt N, Bernreitner K. J Appl Polym Sci 2006;100:283–91.
[19] Li X, Park H-M, Lee J-O, Ha ChS. Polym Eng Sci 2002;42:21–64.
[20] Hong JS, Namkung H, Ahn KH, Lee SJ, Kim C. Polymer 2006;47:3967–75.
[21] Ginzburg VV, Qin F, Paniconi M, Peng G, Jasnow D, Balasz AC. Phys Rev Lett 1999;42:4026–9.
[22] Ahn Y-Ch, Paul DR. Polymer 2006;47:2830–8.
[23] Artzi N, Khatua BB, Narkis M, Siegmann A. Polym Compos 2006;27:15–23.
[24] González I, Eguizábal JI, Nazábal J. J Polym Sci B 2005;43:3611–20.
[25] Dharayia DP, Jana SC. J Polym Sci B 2005;43:3638–51.
[26] Li Y, Shimizu H. Polymer 2004;45:7381–8.
[27] Li Y, Shimizu H. Macromol Rapid Commun 2005;26:710–5.
[28] Zou H, Zhang Q, Tan H, Wang K, Du R, Fu Q. Polymer 2006;47:6–11.
[29] Si M, Araki T, Ade H, Kilcoyne ALD, Fisher R, Sokolov JC, et al. Macromolecules 2006;39:4793–801.

[30] Wan ChI, Zhang Y, Zhang YX, Qiao XY, Teng GM. J Polym Sci B 2004; 42:286–95.
[31] Ren J, Huang Y, Liu Y, Tang X. Polym Test 2005;24:316–23.
[32] Kelnar I, Kotek J, Munteanu BS, Kaprálková L. J Appl Polym Sci 2005; 96:288–93.
[33] Kelnar I, Kotek J, Kaprálková L, Hromádková J, Kratochvíl J. J Appl Polym Sci 2006;100:1571–6.
[34] Yang H, Zhang Q, Gou M, Wang C, Du R, Fu Q. Polymer 2006;47: 2106–15.
[35] Vlasveld DPN, de Jong M, Bersee HEN, Gotsis AD, Picken SJ. Polymer 2005;46:10279–89.
[36] Krishnamoorti R, Yurekli K. Curr Opin Colloid Interface Sci 2001;6: 464–70.
[37] Balakrishnan S, Start PR, Raghavan D, Hudson SD. Polymer 2005;46: 11255–62.
[38] Lazzeri A, Bucknall CB. J Mater Sci 1993;28:6799–806.
[39] Kelnar I, Stephan M, Jakisch L, Fortelný I. J Appl Polym Sci 1997;66: 555–62.